Regioselective Addition of *tert*-BuN≡C to the α Carbon Atom of the Allenyl Ligand in $[Fe_2(CO)_6(\mu\text{-}PPh_2)\{\mu\text{-}\eta^1{:}\eta^2{}_{\alpha,\beta}\text{-}(H)C_\alpha{=}C_\beta{=}C_\gamma H_2\}]$: Formation of $[Fe_2(CO)_6(\mu\text{-}PPh_2)\{\mu\text{-}\eta^1{:}\eta^1\text{-}(tert\text{-}BuN{\equiv}C)C{=}CCH_3\}]$ and $[Fe_2(CO)_6(\mu\text{-}PPh_2)(\mu\text{-}\eta^1{:}\eta^2\text{-}\{tert\text{-}BuNHC(O)CH_2\}C{=}CH_2)]$ via Competitive 1,3-Hydrogen Migration and Hydrolysis of the Reactive Allene-Bridged Intermediate $[Fe_2(CO)_6(\mu\text{-}PPh_2)\{\mu\text{-}\eta^1{:}\eta^1\text{-}(tert\text{-}BuNC)HC{=}C{=}CH_2\}]$

Simon Doherty,*[,†,‡] Graeme Hogarth,[§] Mark Waugh,[‡] Tom H. Scanlan,[‡] William Clegg,[‡] and Mark R. J. Elsegood[‡]

Department of Chemistry, Bedson Building, The University of Newcastle upon Tyne, Newcastle upon Tyne, NE1 7RU, U.K., and Department of Chemistry, University College London, 20 Gordon Street, London WC1H 0AJ, U.K.

Received March 8, 1999

Addition of *tert*-BuN≡C to the $\sigma-\eta$-allenyl complex $[Fe_2(CO)_6(\mu\text{-}PPh_2)\{\mu\text{-}\eta^1{:}\eta^2{}_{\alpha,\beta}\text{-}(H)C_\alpha{=}C_\beta{=}C_\gamma H_2\}]$ results in nucleophilic addition to C_α to give the $\mu\text{-}\eta^1{:}\eta^1$-||-alkyne $[Fe_2(CO)_6(\mu\text{-}PPh_2)\{\mu\text{-}\eta^1{:}\eta^1\text{-}(tert\text{-}BuN{\equiv}C)C{=}CCH_3\}]$ (**2**) and the β,γ-unsaturated amide $[Fe_2(CO)_6(\mu\text{-}PPh_2)(\mu\text{-}\eta^1{:}\eta^2\text{-}\{tert\text{-}BuNHC(O)CH_2\}C{=}CH_2)]$ (**3**). Compounds **2** and **3** are proposed to form via initial nucleophilic attack at C_α to give $[Fe_2(CO)_6(\mu\text{-}PPh_2)\{\mu\text{-}\eta^1{:}\eta^1\text{-}(tert\text{-}BuNC)HC{=}C{=}CH_2\}]$, an unstable zwitterionic allene-bridged intermediate which subsequently undergoes either a 1,3-hydrogen migration to give **2** or hydrolysis by extraneous water to give the β,γ-unsaturated amide **3**. An alternative pathway involving initial nucleophilic attack at C_β to give the metallacyclopentene intermediate $[Fe_2(CO)_6(\mu\text{-}PPh_2)\{\mu\text{-}\eta^1{:}\eta^1\text{-}HC{=}C(tert\text{-}BuNC)CH_2\}]$, followed by 1,3-hydrogen migration *and* C_β to C_α *tert*-BuN≡C migration has been considered. Isotope labeling experiments using $[Fe_2(CO)_6(\mu\text{-}PPh_2)\{\mu\text{-}\eta^1{:}\eta^2{}_{\alpha,\beta}\text{-}(D)C_\alpha{=}C_\beta{=}C_\gamma H_2\}]$ (**1**-d_1) are consistent with a large primary kinetic isotope effect for the transfer of hydrogen between C_α and C_γ. Addition of excess isopropylamine to a hexane solution of **2** gave the amidinium-substituted $\mu\text{-}\eta^1{:}\eta^1$-parallel alkyne derivative $[Fe_2(CO)_6(\mu\text{-}PPh_2)\{\mu\text{-}\eta^1{:}\eta^1\text{-}C(tert\text{-}BuHNC)(NHPr^i)C{=}CCH_3\}]$ (**4**), in near quantitative yield via addition of N−H across the C−N multiple bond. Chloroform solutions of **3** smoothly decarbonylate over several days to afford $[Fe_2(CO)_5(\mu\text{-}PPh_2)(\mu\text{-}\eta^1(C){:}\eta^1(O){:}\eta^2(C)\text{-}\{tert\text{-}BuNHC(O)CH_2\}C{=}CH_2)]$ (**5**), which contains a five-membered metallacycle by virtue of coordination of the amide carbonyl oxygen atom. The single-crystal X-ray structures of **2**, **4**, and **5** are reported.

Introduction

The reactivity of transition metal allenyl complexes ($L_nM{-}C(H){=}C{=}CH_2$) is dominated by the electrophilic character of the C_3 ligand,[1] which readily adds activated X−H bonds (X = O, N, P, S) across the C=C double bond to give allyl,[2] alkenyl,[3] and metallacyclobutene[4] derivatives. While examples of nucleophilic addition to the central carbon atom of mono- and binuclear $\sigma-\eta$-coordinated allenyl ligands are commonplace[2,5] reports of addition to the terminal carbon atoms, C_α and C_γ, remain relatively rare.[6] In comparison to the large body of literature on the reactivity of protic nitrogen,[2,7] oxygen,[2,8] and phosphorus[9] nucleophiles toward either σ- or $\sigma-\eta$-bonded allenyl complexes, their reaction chemistry with soft neutral carbon nucleophiles such as isonitriles is less well developed, somewhat surprising considering that the unsaturated organic product of allenyl−isonitrile coupling could offer immense potential for further functionalization. In addition to direct nucleophilic addition to the coordinated hydro-

† E-mail: simon.doherty@newcastle.ac.uk.
‡ University of Newcastle upon Tyne.
§ University College London.

(1) Doherty, S.; Corrigan, J. F.; Carty, A. J.; Sappa, E. *Adv. Organomet. Chem.* **1995**, *37*, 39. (b) Wojcicki, A. *New J. Chem.* **1994**, *18*, 61.

(2) Breckenridge, S. M.; Taylor, N. J.; Carty, A. J. *Organometallics* **1991**, *10*, 837. (b) Tseng, T.-W.; Wu, I.-T.; Lin, Y.-C.; Chen, C.-T.; Chen, M.-C.; Tsai, Y.-J.; Chen, M.-C.; Wang, Y. *Organometallics* **1991**, *10*, 43. (c) Chen, J.-T.; Hsu, R.-H.; Chen, A.-J. *J. Am. Chem. Soc.* **1998**, *120*, 3243. (d) Baize, M.; Blosser, P. W.; Plantevin, V.; Schimpff, D. G.; Gallucci, J. C.; Wojcicki, A. *Organometallics* **1996**, *15*, 164. (e) Baize, M.; Plantevin, V.; Gallucci, J. C.; Wojcicki, A. *Inorg. Chim. Acta* **1995**, *235*, 1. (f) Hsu, R.-H.; Chen, J.-T.; Lee, G.-H.; Wang, Y. *Organometallics* **1997**, *16*, 1159. (g) Chen, J.-T.; Chen, Y.-K.; Hu, J.-B.; Lee, S.-H.; Wang, Y. *Organometallics* **1997**, *16*, 1476.

(3) Doherty, S.; Elsegood, M. R. J.; Clegg, W.; Scanlan, T. H.; Rees, N. H. *Chem. Commun.* **1996**, 1545.

(4) (a) Casey, C. P.; Nash, J. R.; Yu, C. S.; Selmeczy, A. D.; Chung, S.; Powell, D. R.; Hayashi, R. K. *J. Am. Chem. Soc.* **1998**, *120*, 722. (b) Casey, C. P.; Yi, C.-S. *J. Am. Chem. Soc.* **1992**, *114*, 6597.

10.1021/om9901630 CCC: $18.00
Publication on Web 07/10/1999

carbon, isocyanides can also react via ligand addition/substitution or migratory insertion pathways. For instance, mononuclear (σ-allenyl) palladium and platinum complexes react with RN≡C to afford either (metallovinyl)ketenimine or isonitrile compounds via migratory insertion and ligand substitution, respectively.[10] A survey of the literature reveals just two reports of the reactivity of $\sigma-\eta$-binuclear allenyl complexes with isocyanides. In the first, $[Cp_2Mo_2(CO)_4(\mu\text{-}HC{=}C{=}CH_2]^+$ reacts with *tert*-BuN≡C to give the cyanide addition product $[Cp_2Mo_2(CO)_4(\mu\text{-}HC{\equiv}CCH_2\text{-}CN]$, via carbon−carbon bond formation between C_γ and *tert*-BuN≡C with subsequent elimination of isobutene and H^+,[11] while the second reports that *tert*-BuN≡C undergoes C−C bond formation with C_β in $[Ru_2(CO)_6(\mu\text{-}PPh_2)\{\mu\text{-}\eta^1{:}\eta^2{}_{\alpha,\beta}\text{-}(Ph)C_\alpha{=}C_\beta{=}C_\gamma H_2\}]$ to give the highly electrophilic dimetallacyclopentene $[Ru_2(CO)_6(\mu\text{-}PPh_2)\text{-}\{\mu\text{-}\eta^1{:}\eta^2{}_{\alpha,\beta}\text{-}(Ph)C{=}C(tert\text{-}BuN{\equiv}C)CH_2\}]$,[2a,12] which subsequently reacts with nitrogen- and sulfur-based nucleophiles to give amidinium and thioaminocarbene acetylene complexes, respectively. The highly electrophilic nature of carbon-coordinated isocyanides has prompted us to examine the reaction of isocyanides with the $\sigma-\eta$-binuclear allenyl complex $[Fe_2(CO)_6(\mu\text{-}PPh_2)\text{-}\{\mu\text{-}\eta^1{:}\eta^2{}_{\alpha,\beta}\text{-}(H)C_\alpha{=}C_\beta{=}C_\gamma H_2\}]$ (**1**). Herein we report the first example of regioselective carbon−carbon bond formation between an isonitrile and C_α of a $\sigma-\eta$-coordinated allenyl ligand to give alkyne and $\beta-\gamma$-unsaturated amide bridged complexes via competitive 1,3-hydrogen migration and hydrolysis of the reactive allene-bridged intermediate $[Fe_2(CO)_6(\mu\text{-}PPh_2)\{\mu\text{-}\eta^1{:}\eta^1\text{-}(tert\text{-}BuN{\equiv}C)HC{=}C{=}CH_2\}]$.

Results and Discussion

Addition of *tert*-BuN≡C to the allenyl complex $[Fe_2(CO)_6(\mu\text{-}PPh_2)\{\mu\text{-}\eta^1{:}\eta^2{}_{\alpha,\beta}\text{-}(H)C_\alpha{=}C_\beta{=}C_\gamma H_2\}]$ (**1**) results in nucleophilic addition to C_α to give the $\mu\text{-}\eta^1{:}\eta^1$-||-alkyne-bridged complex $[Fe_2(CO)_6(\mu\text{-}PPh_2)\{\mu\text{-}\eta^1{:}\eta^1\text{-}(tert\text{-}BuN{\equiv}C)C{=}CCH_3\}]$ (**2**) and the α,β-unsaturated amide $[Fe_2(CO)_6(\mu\text{-}PPh_2)(\mu\text{-}\eta^1{:}\eta^2\text{-}\{tert\text{-}BuNHC(O)CH_2\}\text{-}C{=}CH_2)]$ (**3**) (eq 1). Both complexes have been fully

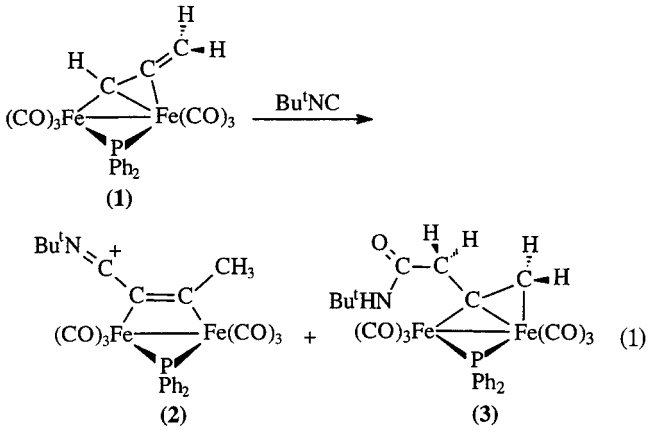

characterized using analytical and spectroscopic techniques and in the case of **2** a single-crystal X-ray structure determination. The pattern of ν(CO) bands in the IR spectrum of **2** is similar to those previously reported for other group 8 alkyne-bridged complexes such as $[Os_2(CO)_6(\mu\text{-}PPh_2)\{\mu\text{-}\eta^1{:}\eta^1\text{-}(tert\text{-}BuN{\equiv}C)C{=}CR\}]$ (R = Ph, Pr^i, Bu^t),[12] $[Fe_2(CO)_6(\mu\text{-}PPh_2)\{\mu\text{-}\eta^1{:}\eta^1\text{-}(tert\text{-}BuN{\equiv}C)C{=}CPh\}]$,[13] and $[Fe_2(CO)_6(\mu\text{-}PPh_2)\{\mu\text{-}\eta^1{:}\eta^1\text{-}(MeO)_3PC{=}CPh\}]$.[14] In the ^{1}H NMR spectrum two singlets at δ 2.09 (3H) and 1.33 (9H) correspond to the CH_3 and *tert*-butyl substituents, respectively, of the bridging hydrocarbon. In the ^{13}C NMR spectrum two broad resonances at δ 214.9 and 213.8 for the carbonyl ligands suggest that **2** undergoes rapid trigonal rotation at 298 K. A low-field singlet at δ 249.6 for the *tert*-BuN≡*C* carbon and two singlets at δ 107.4 and 87.5 for the iron-coordinated carbon atoms of the $\mu\text{-}\eta^1{:}\eta^1$-|| acetylene are consistent with the structure proposed in Scheme 1,[15] which has been confirmed by a single-crystal X-ray structure determination.

The ^{1}H NMR spectrum of **3** contains three distinct multiplets at δ 4.00 (1H), 3.00 (2H), and 2.27 (1H), which correspond to the diastereotopic methylene protons of the bridging hydrocarbon and a nine-proton singlet at δ 1.35 for the *tert*-butyl substituent. The chemicals shifts and coupling patterns of the former resonances are strikingly similar to those reported for the β,γ-unsaturated amides and esters $[Fe_2(CO)_5(\mu\text{-}PPh_2)(\mu\text{-}\eta^1(O){:}\eta^1(C){:}\eta^2(C)\text{-}\{NuC(O)CH_2\}C{=}CH_2)]$,[7b,8a] isolated from the reaction between **1** and the corresponding amine (Nu = NHR) or alcohol (Nu = OR). Notably though, complex **3** is bright yellow, while $[Fe_2(CO)_5(\mu\text{-}PPh_2)(\mu\text{-}\eta^1(O){:}\eta^1(C){:}\eta^2(C)\text{-}\{NuC(O)CH_2\}C{=}CH_2)]$ is deep

(5) (a) Plantevin, V.; Blosser, P. W.; Gallucci, J. C.; Wojcicki, A. *Organometallics* **1994**, *13*, 3651. (b) Blosser, P. W.; Schimpff, D. G.; Gallucci, J. C.; Wojcicki, A. *Organometallics* **1993**, *12*, 1992. (c) Huang, T.-M.; Chen, J.-T.; Lee, G.-H.; Wang, Y. *J. Am. Chem. Soc.* **1993**, *115*, 1170. (d) Su, C.-C.; Chen, J.-T.; Lee, G.-H.; Wang, Y. *J. Am. Chem. Soc.* **1994**, *116*, 4999.

(6) (a) Amouri, H. E.; Gruselle, M. *Chem. Rev.* **1996**, *96*, 1077. (b) Doherty, S.; Elsegood, M. R. J.; Clegg, W.; Mampe, D. *Organometallics* **1996**, *15*, 5302. (c) Doherty, S.; Elsegood, M. R. J.; Clegg, W.; Ward, M. F. W.; Waugh, M. *Organometallics* **1997**, *16*, 4251. (d) McLain, M. D.; Hay, M. S.; Curtis, M. D.; Kampf, J. W. *Organometallics* **1994**, *13*, 4377. (e) Henrick, K.; McPartlin, M.; Deeming, A. J.; Hasso, S.; Manning, P. *J. Chem. Soc., Dalton Trans.* **1982**, 899. (f) Amouri, H.; Besace, Y.; Vaissermann, J.; Ricard, L. *Organometallics* **1997**, *16*, 2160. (g) Amouri, H.; Gruselle, M.; Besace, Y.; Vaissermann, J.; Jaoven, G. *Organometallics* **1994**, *13*, 3, 2244. (h) Bradley, D. H.; Khan, M. A.; Nicholas, K. M. *Organometallics* **1992**, *11*, 2598. (i) Caffyn, A. M.; Nicholas, K. M. *J. Am. Chem. Soc.* **1993**, *115*, 6438.

(7) (a) Doherty, S.; Hogarth, G.; Elsegood, M. R. J.; Clegg, W.; Rees, N. H.; Waugh, M. *Organometallics* **1998**, *17*, 3331, and references therein. (b) Doherty, S.; Elsegood, M. R. J.; Clegg, W.; Waugh, M. *Organometallics* **1996**, *15*, 2688. (c) Chen, A.-J.; Su, C.-C.; Tsai, F.-Y.; Lee, J.-J.; Huang, T.-M.; Yang, C.-S.; Lee, G.-H.; Wang, Y.; Chen, J.-T. *J. Organomet. Chem.* **1998**, *569*, 39.

(8) (a) Doherty, S.; Elsegood, M. R. J.; Clegg, W.; Mampe, D. *Organometallics* **1997**, *16*, 1186. (b) Cheng, Y.-C.; Chen, Y.-K.; Huang, T.-M.; Yu, C.-I.; Lee, G. H.; Wang, Y.; Chen, J.-T. *Organometallics* **1998**, *17*, 2953. (c) Huang, T.-M.; Hsu, R.-H.; Yang, C.-S.; Chen, J.-T.; Lee, G.-H.; Wang, Y. *Organometallics* **1994**, *13*, 3657. (d) Tseng, T.-W.; Wu, I.-Y.; Tsai, J.-H.; Lin, Y.-C.; Chen, D.-T.; Lee, G.-H.; Cheng, M.-C.; Wang, Y. *Organometallics* **1994**, *13*, 3963. (e) Chen, C.-C.; Fan, J.-S.; Lee, G.-H.; Peng, S.-M.; Wang, S.-L.; Lui, R.-S. *J. Am. Chem. Soc.* **1995**, *117*, 2933.

(9) (a) Doherty, S.; Waugh, M.; Elsegood, M. R. J.; Clegg, W. *Organometallics* **1999**, *18*, 679. (b) Blenkiron, P.; Corrigan, J. F.; Carty, A. J.; Doherty, S.; Elsegood, M. R. J.; Clegg, W. *Organometallics* **1997**, *16*, 297.

(10) Wouters, J. M. A.; Klein, R. A.; Elsevier: C. J.; Zoutberg, M. C.; Stam, C. H. *Organometallics* **1993**, *12*, 3864.

(11) Meyer, A.; McCabe, D. J.; Curtis, M. D. *Organometallics* **1987**, *6*, 1491.

(12) Cherkas, A. A.; Hadj-Bagheri, N.; Carty, A. J.; Sappa, E.; Pellinghelli, M. V.; Tiripicchio, A. *Organometallics* **1990**, *9*, 1887.

(13) Carty, A. J.; Mott, G. M.; Taylor, N. J. *J. Organomet. Chem.* **1981**, *212*, C54.

(14) Wong, Y.-S.; Paik, H.-N.; Cheih, P. C.; Carty, A. J. *J. Chem. Soc., Chem. Commun.* **1975**, 309.

(15) Cherkas, A. A.; Breckenridge, S. M.; Carty, A. J. *Polyhedron* **1992**, *11*, 1075.

Scheme 1

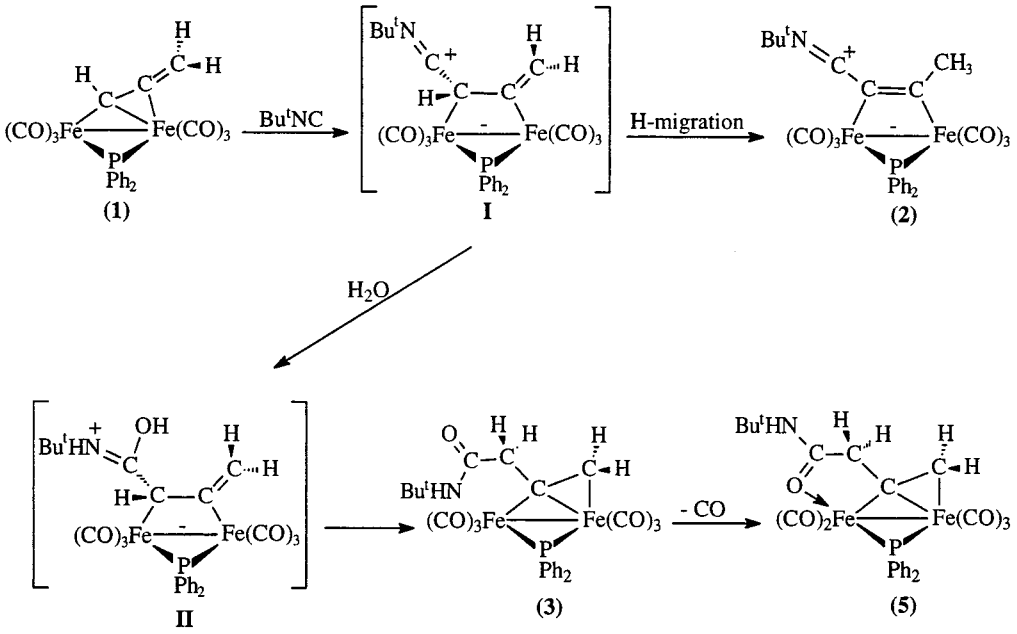

red. The alkenyl protons appear as doublets of doublets with one large ($^2J_{PH}$ = 10.1 Hz) and one small geminal ($^2J_{HH}$ = 2.8 Hz) coupling constant, while the remaining diastereotopic methylene protons exhibit one large geminal coupling ($^2J_{HH}$ = 12.8 Hz). The most noteworthy feature of the ^{13}C NMR spectrum of **3** in comparison to that of $[Fe_2(CO)_5(\mu\text{-}PPh_2)(\mu\text{-}\eta^1(O):\eta^2(C)\text{-}\{NuC(O)CH_2\}C{=}CH_2)]$ (Nu = OR, NRH)[7c,8a] lies in the carbonyl region. The ^{13}C NMR spectrum of the latter complexes generally contain one exchange-broadened resonance and two distinct doublets, in the low-field region, associated with the $Fe(CO)_3$ fragment undergoing trigonal rotation and the two carbonyl ligands attached to the ester/amide-coordinated iron atom, respectively. In contrast, the ^{13}C NMR spectrum of **3** contains a single sharp carbonyl resonance ($\sim\delta$ 212) at room temperature, which we initially associated with all six carbonyl ligands, suggesting that trigonal rotation and $\sigma-\eta$-windshield-wiper exchange are both rapid at 298 K.[16] We have previously monitored the fluxionality of $[Fe_2(CO)_6(\mu\text{-}PPh_2)(\mu\text{-}\eta^1:\eta^2\text{-}CH{=}CH_2)]$ by variable-temperature ^{13}C NMR spectroscopy and shown exchange via the windshield-wiper process to be slow at 300 K, as evidenced by the presence of two distinct CO resonances.[16a] Large differences in the free energy of activation for windshield-wiper exchange have been attributed to ground-state effects.[17] Thus complexes in which the $M-C_\alpha$ bond lengths are similar and the $M-C_\beta$ bond lengths elongated are highly fluxional, requiring only minor distortions to reach the symmetrical transition state for exchange. More light was shed on the fluxionality of **3** upon running low-temperature ^{13}C NMR spectra. At 193 K in CD_2Cl_2 three distinct doublets are seen, each with a quite different $^2J_{PC}$ coupling constant ($^2J_{PC}$ = 10.0, 24.0, 32.0 Hz), together with a single exchange-broadened signal, which corresponds to exchange of a similar set of three resonances. Qualitatively, at 193 K interchange involving the σ- and π-bonding interactions via a windshield-wiper motion is slow, as is trigonal rotation at one of the $Fe(CO)_3$ units. Nondegenerate trigonal rotations in $\sigma-\eta^2$-alkenyl complexes is commonplace, with the lowest energy process usually associated with the η^2-coordinated iron.[18] Upon raising the temperature, the broad resonance sharpens such that it appears as a sharp singlet, while the three distinct doublets broaden until, at room temperature, they disappear into the baseline. Unfortunately, we have not been able to collect spectra at higher temperature due to facile loss of CO. However, it should be noted that the average chemical shift of the three distinct low-temperature doublets is δ 209.4, and thus a time-averaged singlet for all six carbonyls would be expected to appear at $\sim\delta$ 210.9. Thus, it is clear that even at room temperature windshield-wiper motion is slow on the NMR time scale. The remainder of the ^{13}C spectrum of **3** compares closely with that of the related β,γ-unsaturated derivatives $[Fe_2(CO)_5(\mu\text{-}PPh_2)(\mu\text{-}\eta^1(O):\eta^1(C):\eta^2(C)\text{-}\{NuC(O)CH_2\}C{=}CH_2)]$. Three distinctive resonances are seen: two at low field, one in the region commonly associated with C_α of $\mu\text{-}\eta^1:\eta^1$-alkenyl ligands (δ 180.4, $^2J_{PC}$ = 21.7 Hz), the other a ketonic carbonyl resonance at δ 169.3, and one at high field (δ 67.3) which corresponds to C_β of the alkenyl ligand.

Isotope labeling studies using $[Fe_2(CO)_6(\mu\text{-}PPh_2)\{\mu\text{-}\eta^1:\eta^2{}_{\alpha,\beta}\text{-}(D)C_\alpha{=}C_\beta{=}C_\gamma H_2\}]$ (**1**-d_1) and *tert*-BuN≡C gave $[Fe_2(CO)_6(\mu\text{-}PPh_2)\{\mu\text{-}\eta^1:\eta^1\text{-}(tert\text{-}BuN{\equiv}C)C{=}CCH_2\}]$ (**2**-d_1), identified in the $^1H\{^{31}P\}$ NMR spectrum by a triplet ($^2J_{HD}$ = 2.2 Hz) at 16.8 ppb lower frequency (8.4 Hz at 500 MHz) due to the deuterium isotope shift of the methyl resonance, and $[Fe_2(CO)_6(\mu\text{-}PPh_2)(\mu\text{-}\eta^1:\eta^2\text{-}$

(16) (a) MacLaughlin, S. A.; Doherty, S. Taylor, N. J.; Carty, A. J. *Organometallics* **1992**, *11*, 4315. (b) Xue, Z.; Sieber, W. J.; Knobler, C. B.; Kaesz, H. D. *J. Am. Chem. Soc.* **1990**, *112*, 1825. (c) Shapley, J. R. Richter, S. I.; Tachikawa, M.; Keister, J. B. *J. Organomet. Chem.* **1975**, *94*, C43. (d) Farrugia, L.; Chi, Y.; Tu, W.-C. *Organometallics* **1993**, *12*, 1616. (e) Casey, C. P.; Marder, S. R.; Adams, B. R. *J. Am. Chem. Soc.* **1985**, *107*, 7700, and references therein.

(17) Hogarth, G.; Lavender, M. H.; Shukri, K. *J. Organomet. Chem.* **1997**, *527*, 247.

(18) Patin, H.; Mignami, G.; Benoit, A.; McGlinchey, M. J. *J Chem. Soc., Dalton Trans.* **1981**, 1278.

Scheme 2

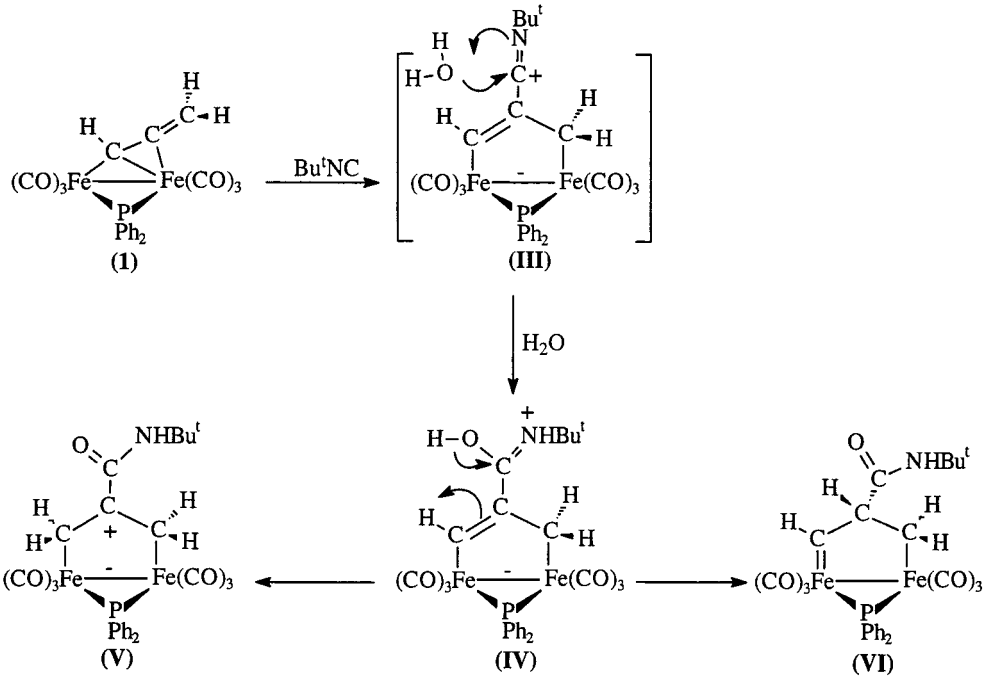

(*tert*-BuNHC(O)CHD}C=CH_2)] (**3**-d_1), identified by two broad resonances in the ^{2}H NMR spectrum at δ 4.02 and 3.00. Moreover, a similar ^{2}H NMR spectrum was obtained for **3**-d_1 isolated from an isotope labeling experiment using protio-**1**, purified by column chromatography using alumina deactivated with 6% D_2O, prior to addition of *tert*-BuN≡C. The isotopic composition of **2**-d_1 supports the mechanism shown in Scheme 1, whereby regiospecific carbon−carbon bond formation between *tert*-BuN≡C and C_α of the bridging allenyl ligand is followed by 1,3-hydrogen migration, while the formation **3**-d_1, with deuterium located solely on C_α of the original allenyl fragment, is as expected for a reaction involving hydrolysis of a common intermediate (vide infra). These labeling studies are consistent with a pathway involving initial nucleophilic attack of *tert*-BuN≡C at C_α of **1** to give [$Fe_2(CO)_6$(μ-PPh_2){μ-η^1:η^1-(*tert*-BuNC)HC=C=CH_2}] (**I**), an unstable zwitterionic allene-bridged intermediate, which undergoes either a 1,3-hydrogen migration to give **2** or rapid hydrolysis by extraneous water to give the β,γ-unsaturated amide **3** (Scheme 1).

The mechanism proposed in Scheme 1 is based on our previous observations of C−C_α and P−C_α bond-forming reactions of **1**.[3,6c,8a,26] In particular, we have isolated the zwitterionic allene-bridged [$Fe_2(CO)_6$(μ-SCy){μ-η^1:η^1-[$P(OMe)_3$]HC=C=CH_2}], from the reaction between [$Fe_2(CO)_6$(μ-SCy){μ-η^1:$\eta^2_{\alpha,\beta}$-(H)C_α=C_β=$C_\gamma H_2$}] and trimethyl phosphite.[19] Even though labeling studies are consistent with the pathway described in Scheme 1, we must consider an alternative pathway for the formation of **2** involving initial nucleophilic addition to C_β, as previously described by Carty and co-workers for [Ru_2-$(CO)_6$(μ-PPh_2){μ-η^1:$\eta^2_{\alpha,\beta}$-(Ph)C_α=C_β=$C_\gamma H_2$}], followed by 1,3-hydrogen migration *and* C_β to C_α *tert*-BuN≡C migration. If this pathway were operative, we might expect to obtain additional products resulting from hydrolysis of the *tert*-BuN≡C coordinated metallacyclopentene intermediate [$Fe_2(CO)_6$(μ-PPh_2){μ-η^1:η^1-HC=C(*tert*-BuNC)CH_2}] (**III**), for instance the organo-amide derivatives **V** and/or **VI** (Scheme 2). No such compounds have been isolated. However, since **2** is stable with respect to hydrolysis there is no reason to expect an intermediate such as **III** to undergo hydrolysis, and thus on the basis of these considerations it is difficult to eliminate the involvement of a metallacyclopentene intermediate. The reaction between **1** and *tert*-BuN≡C has been monitored by ^{13}C and ^{1}H NMR spectroscopy, and while resonances consistent with the formation of an allene-bridged intermediate have been identified, the low concentration of this species in solution has prevented its isolation and characterization. Thus, although we cannot exclude a pathway involving nucleophilic addition to C_β, we favor initial formation of an allene-bridged intermediate via addition to C_α.

In spite of the above comment, rapid hydrolysis of an intermediate such as **I** is not surprising since carbon-coordinated isonitriles have previously been shown to be highly electrophilic, reacting with protic nitrogen- and sulfur-based nucleophiles to afford elaborate di-

(19) Doherty, S.; Elsegood, M. R. J.; Clegg, W. Unpublished results.
(20) (a) Cherkas, A. A.; Carty, A. J.; Sappa, E.; Pellinghelli, M. A.; Tiripicchio, A. *Inorg. Chem.* **1987**, *26*, 3201. (b) MacLaughlin, S. A.; Johnson, J. P.; Taylor, N. J.; Carty, A. J.; Sappa, E. *Organometallics* **1983**, *2*, 352.
(21) Bent, H. A. *Chem. Educ.* **1960**, *37*, 616.
(22) Merenyi, R. Iminium Salts in Organic Chemistry, Part 1. In *Advances in Organic Chemistry: Methods and Results*; Bohme, H., Viehe, H. G., Eds.; Wiley: New York, 1976; Vol. 9, p 1.
(23) (a) Biradha, K.; Desiraju, G. R.; Braga, D.; Grepioni, F. *Organometallics* **1996**, *15*, 1285. (b) Braga, D.; Grepioni, F. *Chem. Commun.* **1996**, 571. (c) Braga, D.; Grepioni, F.; Biradha, K.; Pedireddi, V. R.; Desiraju, G. R. *J. Am.Chem. Soc.* **1995**, *117*, 3156.
(24) (a) Carty, A. J.; MacLaughlin, S. A.; Nicciarone, D. *In Phosphorus-31 NMR Spectroscopy in Stereochemical Analysis: Organic Compounds and Metal Complexes*; Verkade, J. G., Quinn, L. D., Eds.; VCH: New York, 1987; Chapter 16, pp 54−619. (b) Carty, A. J. *Adv. Chem Ser.* **1982**, *196*, 163.
(25) Hogarth, G.; Lavender, M. H. *J. Chem. Soc., Dalton Trans.* **1994**, 3389.
(26) Doherty, S.; Elsegood, M. R. J.; Clegg, W.; Rees, N. H.; Scanlan, T. H.; Waugh, M. *Organometallics* **1997**, *16*, 3221.

functional unsaturated hydrocarbyl ligands.[13,20] For instance, the dimetallacyclopentene $[Ru_2(CO)_6(\mu\text{-}PPh_2)\{\mu\text{-}\eta^1\text{:}\eta^1\text{-}PhC{=}C(tert\text{-}BuN{\equiv}C)CH_2\}]$ reacts with ethanethiol and ethylamine to give $[Ru_2(CO)_6(\mu\text{-}PPh_2)\{\mu\text{-}\eta^1\text{:}\eta^1\text{-}PhC{=}C[\{C(EtNH)(NH\text{-}tert\text{-}Bu)\}]CH_2\}]$ and $[Ru_2(CO)_6(\mu\text{-}PPh_2)\{\mu\text{-}\eta^1\text{:}\eta^1\text{-}PhC{=}C[\{C(EtS)(NH\text{-}tert\text{-}Bu)\}]CH_2\}]$, respectively,[2a] while $[Os_2(CO)_6(\mu\text{-}PPh_2)\{\mu\text{-}\eta^1\text{:}\eta^1\text{-}(tert\text{-}BuN{\equiv}C)C{=}CPh\}]$ reacts with butanethiol to give the dimetallacyclobutene $[Os_2(CO)_6(\mu\text{-}PPh_2)\{\mu\text{-}\eta^1\text{:}\eta^2\text{-}(NH\text{-}tert\text{-}Bu)(S\text{-}n\text{-}Bu)C{-}C{=}CPh\}]$.[20a] In a similar manner, we suggest that nucleophilic addition of H_2O to **I** generates $[Fe_2(CO)_6(\mu\text{-}PPh_2)\{\mu\text{-}\eta^1\text{:}\eta^1\text{-}(tert\text{-}BuNH)C(OH)HCC{=}CH_2\}]$ (**II**), which is unstable and rapidly undergoes an organometallic keto−enol tautomerisation to give the β,γ-unsaturated amide $[Fe_2(CO)_6(\mu\text{-}PPh_2)(\mu\text{-}\eta^1\text{:}\eta^2\text{-}\{tert\text{-}BuNHC(O)CH_2\}C{=}CH_2)]$ (**3**) (Scheme 1). In a competitive experiment, the reaction between *tert*-BuN≡C and $[Fe_2(CO)_6(\mu\text{-}PPh_2)\{\mu\text{-}\eta^1\text{:}\eta^2{}_{\alpha,\beta}\text{-}(H)C_\alpha{=}C_\beta{=}C_\gamma H_2\}]$ (**1**-d_0) and $[Fe_2(CO)_6(\mu\text{-}PPh_2)\{\mu\text{-}\eta^1\text{:}\eta^2{}_{\alpha,\beta}\text{-}(D)C_\alpha{=}C_\beta{=}C_\gamma H_2\}]$ (**1**-d_1) gave **2** and **3** as 1:2.96 and 1:0.61 mixtures, respectively, indicating that **1**-d_1 reacts with *tert*-BuN≡C primarily via hydrolysis, whereas its protio derivative, **1**-d_0, preferentially undergoes 1,3-hydrogen migration. Similar ratios have been obtained from three separate experiments. Such a large difference in product distribution arising from isotopic substitution is consistent with a large primary kinetic isotope effect (∼4.9) and suggestive of a symmetrical transition state for the transfer of hydrogen between C_α and C_γ.

The carbon-coordinated isonitrile in **2** shows a reactivity similar to that previously reported for the bi- and trinuclear derivatives $[Os_2(CO)_6(\mu\text{-}PPh_2)\{\mu\text{-}\eta^1\text{:}\eta^1\text{-}(tert\text{-}BuN{\equiv}C)C{=}CPh\}]$[13,20a] and $[Os_3(CO)_9(\mu\text{-}PPh_2)\{\mu\text{-}\eta^1\text{:}\eta^1\text{:}\eta^2\text{-}(tert\text{-}BuN{\equiv}C)C{=}CPh\}]$,[20b] respectively. Addition of excess isopropylamine to a hexane solution of **2** results in immediate precipitation of a yellow solid, the amidinium-substituted $\mu\text{-}\eta^1\text{:}\eta^1$-parallel alkyne complex $[Fe_2(CO)_6(\mu\text{-}PPh_2)\{\mu\text{-}\eta^1\text{:}\eta^1\text{-}C(tert\text{-}BuHNC)(NH\text{-}Pr^i)C{=}CCH_3\}]$ (**4**), formed via addition of the primary amine across the C≡N multiple bond (eq 2). The pattern

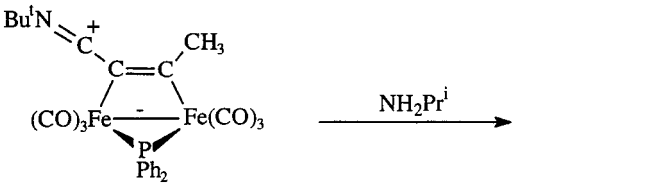

(**2**)

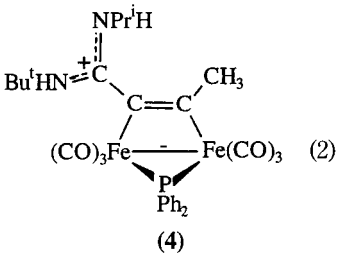

(**4**) (2)

and intensities of ν(CO) bands closely resemble that for the osmium derivative $[Os_2(CO)_6(\mu\text{-}PPh_2)\{\mu\text{-}\eta^1\text{:}\eta^1\text{-}(tert\text{-}BuN{\equiv}C)C{=}CPh\}]$, although the frequencies for **4** are significantly lower than those of their heavier counterparts, which presumably reflects greater π-back-bonding to CO in the iron complex. In the ^{1}H NMR spectrum two doublets at δ 1.20 and 1.05 correspond to the diastereotopic methyl groups of the isopropyl substituent, while the N-*H* protons appear as well-separated resonances at δ 4.81 and 3.85. In the ^{13}C NMR spectrum two doublets at δ 121.1 ($^2J_{PC}$ = 8.9 Hz) and 161.0 ($^2J_{PC}$ = 11.3 Hz) are in the range expected for a parallel acetylene complex, with carbene-like character. In the carbonyl region three distinct doublets at δ 217.6, 216.0, and 211.6, each with vastly disparate coupling constants, and one exchange-broadened resonance at δ 215.8 correspond to the two $Fe(CO)_3$ fragments. The observation of three well-resolved signals indicates that trigonal rotation of one of the $Fe(CO)_3$ fragments is unusually slow at 298 K, most likely at the iron atom σ-bonded to the amidinium-substituted carbon, which would experience unfavorable steric interactions between CO and the bulky substituents on the nitrogen atoms of the amidinium-substituted carbon. The broad resonance at δ 215.8 corresponds to the remaining $Fe(CO)_3$ fragment, which undergoes trigonal rotation on the NMR time scale. Full details of the molecular structure of **4** have been obtained from a single-crystal X-ray analysis (vide infra). Notably, chloroform solutions of **2** are stable with respect to hydrolysis in the presence of added water.

The chemical reactivity of **3** also supports the formulation shown in Scheme 1. Upon standing under an inert atmosphere, chloroform solutions of **3** smoothly decarbonylate over several days to afford $[Fe_2(CO)_5(\mu\text{-}PPh_2)(\mu\text{-}\eta^1(C)\text{:}\eta^1(O)\text{:}\eta^2(C)\text{-}\{tert\text{-}BuNHC(O)CH_2\}C{=}CH_2)]$ (**5**), isolated as deep red crystals in near quantitative yield, identified in the first instance using spectroscopic data and later by a single-crystal X-ray structure determination (vide infra). This transformation is conveniently followed by ^{1}H NMR spectroscopy, which clearly shows the appearance of four new diastereotopic methylene resonances at δ 4.23, 3.18, 2.78, and 2.21, associated with the hydrocarbyl bridging ligand of **5**. With the exception of the carbonyl region, which contains a singlet and two doublets for the $Fe(CO)_3$ and $Fe(CO)_2$ fragments, respectively, the ^{13}C NMR spectra of **3** and **5** are closely similar, the latter containing two low-field resonances at δ 168.9 and 183.1 for C_α and the amide carbonyl carbon and a high-field doublet at δ 63.2 ($^2J_{PC}$ = 8.7 Hz), which corresponds to C_β.

X-ray Structures of 2, 4, and 5. A single-crystal X-ray structure analysis was carried out to determine the precise structural features of **2**, the result of which is shown in Figure 1, with selected bond lengths and angles listed in Table 1. The molecular structure clearly shows two iron atoms bridged by a zwitterionic *tert*-BuN≡C-substituted parallel alkyne with σ-interactions to C(2) (Fe(1)−C(2) = 1.991(2) Å) and C(3) (Fe(2)−C(3) = 2.034(2) Å) and a short C(2)−C(3) bond length of 1.347(3) Å, which compares with the corresponding bond length of 1.33(2) Å in $[Fe_2(CO)_6(\mu\text{-}PPh_2)\{\mu\text{-}\eta^1\text{:}\eta^1\text{-}(tert\text{-}BuN{\equiv}C)C{=}CPh\}]$.[13] The four atoms of the dimetallacyclobutene fragment, Fe(1), Fe(2), C(2), and C(3), are essentially planar with a maximum deviation from the best least-squares plane of 0.028 Å. The phosphido ligand asymmetrically bridges the two iron atoms (Fe(1)−P(1) = 2.2067(7); Fe(2)−P(1) = 2.2124(7) Å) and lies perpendicular to the dimetallacyclobutene ring with a dihedral angle of 92.3° between the plane of the tri-

Table 1. Selected Bond Distances (Å) and Angles (deg) for Compounds 2, 4, and 5

compound 2		compound 4		compound 5	
Fe(1)−Fe(2)	2.6744(5)	Fe(1)−Fe(2)	2.6656(4)	Fe(1)−Fe(2)	2.6180(3)
Fe(1)−C(2)	1.991(2)	Fe(1)−C(2)	2.0201(16)	Fe(1)−C(2)	1.9511(16)
Fe(2)−C(3)	2.034(2)	Fe(2)−C(3)	2.0460(16)	Fe(2)−C(1)	2.1690(16)
Fe(1)−P(1)	2.2067(7)	Fe(1)−P(1)	2.2001(5)	Fe(2)−C(2)	2.1262(15)
Fe(2)−P(1)	2.2124(7)	Fe(2)−P(1)	2.2106(5)	Fe(1)−P(1)	2.1547(5)
C(1)−C(2)	1.506(3)	C(1)−C(2)	1.509(2)	Fe(2)−P(1)	2.2715(5)
C(2)−C(3)	1.347(3)	C(2)−C(3)	1.326(2)	Fe(1)−O(1)	2.0237(12)
C(3)−C(4)	1.386(3)	C(3)−C(4)	1.477(2)	C(1)−C(2)	1.394(2)
C(4)−N(1)	1.149(3)	C(4)−N(1)	1.322(2)	C(2)−C(3)	1.524(2)
N(1)−C(5)	1.469(3)	C(4)−N(2)	1.329(2)	C(3)−C(4)	1.497(2)
		N(1)−C(5)	1.475(2)	C(4)−O(1)	1.254(2)
		N(2)−C(8)	1.490(2)		
Fe(1)−P(1)−Fe(2)	75.48(2)	Fe(1)−P(1)−Fe(2)	74.365(16)	Fe(1)−P(1)−Fe(2)	72.469(16)
P(1)−Fe(1)−C(2)	80.51(7)	P(1)−Fe(1)−C(2)	82.41(5)	Fe(1)−C(2)−C(1)	130.34(12)
P(1)−Fe(2)−C(3)	79.89(7)	P(1)−Fe(2)−C(3)	80.85(5)	C(1)−C(2)−C(3)	117.75(14)
C(2)−C(3)−C(4)	125.3(2)	C(2)−C(3)−C(4)	122.73(15)	C(2)−C(3)−C(4)	108.52(13)
C(3)−C(4)−N(1)	174.5(3)	C(3)−C(4)−N(1)	121.17(15)	C(3)−C(4)−O(1)	118.16(15)
C(4)−N(1)−C(5)	170.0(2)	C(3)−C(4)−N(2)	117.24(15)		
		C(4)−N(1)−C(5)	126.32(14)		
		C(4)−N(2)−C(8)	130.67(15)		
		N(1)−C(4)−N(2)	121.58(15)		

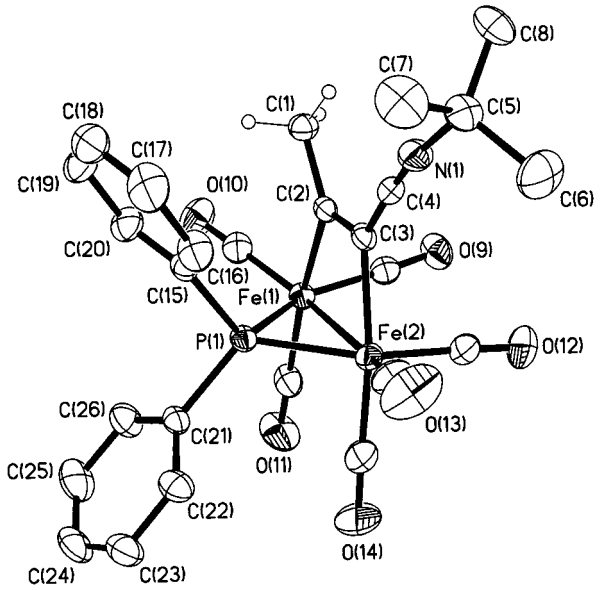

Figure 1. Molecular structure of $[Fe_2(CO)_6(\mu\text{-}PPh_2)\{\mu\text{-}\eta^1\text{:}\eta^1\text{-}(tert\text{-}BuN{\equiv}C)C{=}CCH_3\}]$ (**2**). Phenyl, *tert*-butyl, and methyl hydrogen atoms have been omitted. Carbonyl carbons have the same numbers as oxygen atoms. Ellipsoids are at the 50% probability level.

angular Fe_2P core and that defined by Fe(1), Fe(2), C(2), and C(3). The N(1)−C(4) bond length of 1.149(2) Å is in the range expected for a carbon−nitrogen triple bond, which indicates that the contribution from resonance structure **B** is substantially greater than that from **A**. The C(3)−C(4) bond length of 1.386(3) Å is longer than expected for a carbon−carbon double bond, which is suggestive of a minor contribution from the alternative keteneimine−carbene resonance form **C**, also supported by the difference in Fe−C bond lengths, Δ, of 0.043 Å (Fe(1)−C(2) = 1.991(2) Å; Fe(2)−C(3) = 2.034(2) Å).[15] The carbon-coordinated isocyanide is essentially linear (C(3)−C(4)−N(1) = 174.5(3)°; C(4)−N(1)−C(5) = 170.0(2)°), as expected for sp-hybridized carbon and nitrogen atoms. Both iron atoms support three carbonyl ligands, one trans to the phosphido bridge, one trans to the bridging acetylene, and the remaining one trans to the Fe−Fe bond.

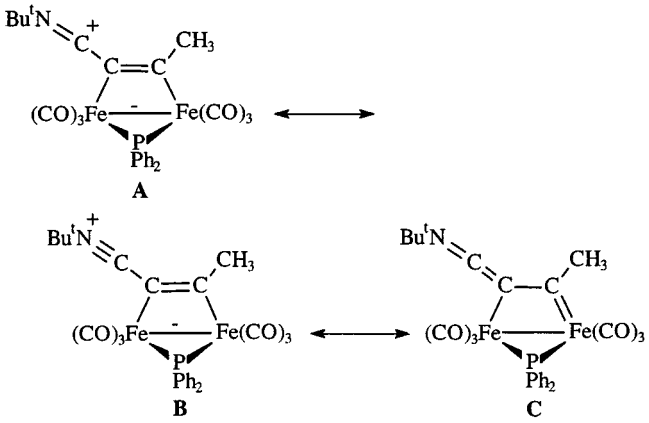

A single-crystal X-ray structure determination of **4** was carried out to confirm the proposed formulation and to compare with that of **2**. A perspective view of the molecular structure is shown in Figure 2, and a selection of bond lengths and angles is listed in Table 1. The two iron atoms in **4** are separated by a distance of 2.6656(4) Å and asymmetrically bridged by an amidinium-functionalized parallel alkyne, *σ*-bonded to C(2) (Fe(1)−C(2) 2.0201(16) Å) and C(3) (Fe(2)−C(3) = 2.0469(16) Å). Notably, the difference in Fe−C bond lengths, Δ, of 0.0268 Å in **4** is substantially smaller than that in **2** (0.043 Å), which possibly reflects a smaller contribution from the carbene resonance structure. As for **2** the four atoms of the dimetallacylobutene ring are essentially perpendicular to the plane containing Fe(1), C(2), and P(1), forming a dihedral angle of 94.1°. The coordination sphere of both iron atoms is completed by three carbonyl ligands which adopt an eclipsed conformation. The C(2)−C(3) bond length of 1.326(2) Å is similar to C−C distances in a number of dimetallacyclobutenes, including **2**. The C(3)−C(4) bond length of 1.477(2) Å is typical of a single bond between sp^2-hybridized carbon atoms,[21] and the C(4)−N(1) (1.322(2) Å) and C(4)−N(2) (1.329(2) Å) distances are essentially identical, consistent with multiple bonding involving lone pairs on sp^2-hybridized nitrogen atoms

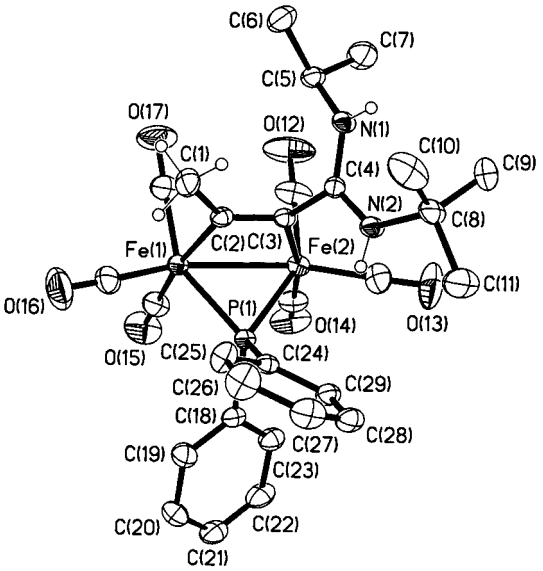

Figure 2. Molecular structure of $[Fe_2(CO)_6(\mu\text{-}PPh_2)\{\mu\text{-}\eta^1{:}\eta^1\text{-}C(tert\text{-}BuHNC)(NHPr^i)C{=}CCH_3\}]$ (**4**). Phenyl and methyl hydrogen atoms have been omitted. Carbonyl carbons have the same numbers as oxygen atoms. Ellipsoids are at the 50% probability level.

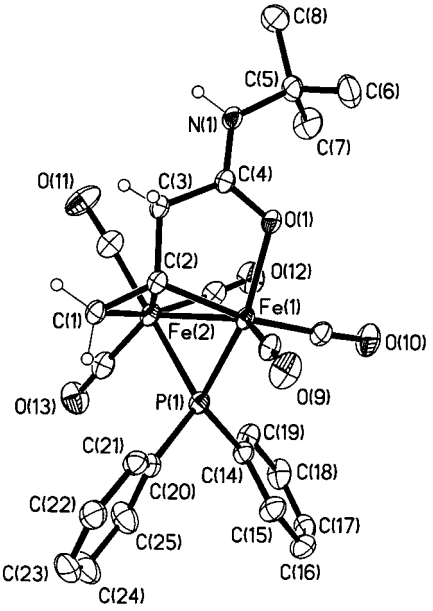

Figure 3. Molecular structure of $[Fe_2(CO)_6(\mu\text{-}PPh_2)(\mu\text{-}\eta^1{:}\eta^2\text{-}\{tert\text{-}BuNHC(O)CH_2\}C{=}CH_2)]$ (**5**). Phenyl, isopropyl, and methyl hydrogen atoms have been omitted. Carbonyl carbons have the same numbers as oxygen atoms. Ellipsoids are at the 50% probability level.

and an empty p-orbital on C(4).[22] The planar nature of N(1), N(2), and C(4) (sum of angles 359.4°, 360.0°, and 360.0°, respectively) supports this interpretation of bonding in the amidinium fragment. The planes defined by the metallacycle and N(2), C(4), and N(1) are close to perpendicular and form a dihedral angle of 76.4°, presumably to minimize steric interactions.

The molecular structure of **5** is shown in Figure 3, and a selection of relevant bond lengths and angles is listed in Table 1. Interestingly, individual diiron fragments are associated through weak intermolecular H-bonding interactions between the N−H and the oxygen atom of a carbonyl group on the amide coordinated iron atom of a neighboring diiron unit (N- - -O = 3.182 Å and an N−H- - -O angle of 141°), to form symmetric dimers. These hydrogen-bonding interactions do not propagate through the crystal but are restricted to individual dimeric units. Braga and co-workers have recently used the Cambridge Structural Database to undertake a systematic examination of hydrogen bond patterns in organometallic crystals and found that CO ligands can behave as hydrogen bond acceptors from donors such as O−H, N−H, and even C−H.[23] As expected, the two iron atoms in **5** are asymmetrically bridged by a phosphido ligand (Fe(1)−P(1) = 2.1547(5); Fe(2)−P(1) = 2.2715(5) Å)[24] with one of the iron atoms, Fe(2), carrying three carbonyl ligands, while the other, Fe(1), carries two. Coordination of the ester carbonyl oxygen atom, O(1), to Fe(1) forms a five-membered metallacycle, such that O(1) is trans to P(1) (O(1)−Fe(1)−P(1) = 153.48(4)°) and with Fe−O (Fe(1)−O(1) = 2.0237(12) Å) and C−O (C(1)−O(1) = 1.254(2) Å) bond lengths similar to those previously reported for $[Fe_2(CO)_4(\mu\text{-}PPh_2)(\mu\text{-dppm})\{\eta^2\text{-}C(CO_2Me){=}CHC(OMe){=}O\}]$.[25] The remainder of the coordination sphere of Fe(1) is completed by two carbonyl ligands and a σ-interaction to the α-carbon atom of the bridging β,γ-unsaturated amide (Fe(1)−C(2) = 1.9511(16) Å). The C(1)−C(2) bond length of 1.394(2) Å corresponds to a bond order of between 1 and 2 and is consistent with the elongation previously reported for $\sigma\text{-}\eta^2$-coordinated alkenyl ligands (Fe(2)−C(1) = 2.1690(16) Å; Fe(2)−C(2) = 2.1262(15) Å).[16]

In conclusion, $[Fe_2(CO)_6(\mu\text{-}PPh_2)\{\mu\text{-}\eta^1{:}\eta^2{}_{\alpha,\beta}\text{-}(H)C_\alpha{=}C_\beta{=}C_\gamma H_2\}]$ (**1**) reacts with *tert*-BuN≡C via regiospecific C−C bond formation with C_α of the $\sigma\text{-}\eta$-allenyl ligand to give the parallel alkyne-bridged $[Fe_2(CO)_6(\mu\text{-}PPh_2)\{\mu\text{-}\eta^1{:}\eta^1\text{-}(tert\text{-}BuN{\equiv}C)C{=}CCH_3\}]$ (**2**) and the β,γ-unsaturated amide $[Fe_2(CO)_6(\mu\text{-}PPh_2)(\mu\text{-}\eta^1{:}\eta^2\text{-}\{tert\text{-}BuNHC(O)CH_2\}C{=}CH_2)]$ (**3**), respectively. Compounds **2** and **3** are proposed to form via initial nucleophilic attack at C_α to give $[Fe_2(CO)_6(\mu\text{-}PPh_2)\{\mu\text{-}\eta^1{:}\eta^1\text{-}(tert\text{-}BuNC)HC{=}C{=}CH_2\}]$, an unstable zwitterionic allene-bridged intermediate, which subsequently undergoes either a 1,3-hydrogen migration to give **2** or hydrolysis by extraneous water to give the β,γ-unsaturated amide **3**. We have not been able to unequivocally exclude an alternative pathway for the formation of **2** involving initial nucleophilic addition to C_β followed by 1,3-hydrogen migration *and tert*-BuN≡C migration. This is the first example of addition of a carbon nucleophile at C_α of a coordinated allenyl ligand and contrasts sharply with previous reports of addition to the β- and γ-carbon atoms of binuclear allenyl complexes and the migratory insertion reactions of mononuclear σ-allenyl derivatives.

Experimental Section

General Procedures. Unless otherwise stated all manipulations were carried out in an inert atmosphere glovebox or by using standard Schlenk line techniques. Diethyl ether and hexane were distilled from Na/K alloy; tetrahydrofuran was distilled from potassium and dichloromethane from CaH_2. $CDCl_3$ was predried with CaH_2, vacuum transferred, and stored over 4 Å molecular sieves. Reactions were monitored by thin-layer chromatography (Baker flex silica gel, 1B-F).Variable-temperature ^{13}C NMR spectra were recorded on a JEOL LAMBDA 500. Column chromatography was carried out with alumina purchased from Aldrich Chemical Co. and

Table 2. Summary of Crystal Data and Structure Determination for Compounds 2, 4, and 5

	2	4	5
molecular formula	$C_{26}H_{22}Fe_2NO_6P_2$	$C_{29}H_{31}Fe_2N_2O_6P$	$C_{25}H_{24}Fe_2NO_6P$
fw	587.12	646.23	577.12
cryst size, mm	0.11 × 0.20 × 0.48	0.16 × 0.26 × 0.50	0.28 × 0.29 × 0.54
temperature, K	173	160	160
cryst syst	monoclinic	monoclinic	triclinic
space group	*C*2/*c*	$P2_1/c$	$P\bar{1}$
a, Å	28.981(2)	9.4537(6)	8.5433(5)
b, Å	13.2742(11)	19.1346(11)	11.6773(7)
c, Å	15.5704(14)	17.1325(10)	13.4130(7)
α, deg			91.276(2)
β, deg	115.623(2)	102.218(4)	99.797(2)
γ, deg			103.431(2)
V, Å^3	5400.8(8)	3028.9(3)	1279.87(13)
Z	8	4	2
D_{calcd}, g cm^{-3}	1.444	1.417	1.498
μ, mm^{-1}	1.173	1.053	1.236
F(000)	2400	1336	592
θ range, deg	1.6−28.8	1.6−29.2	1.5−28.84
max indices: *h*, *k*, *l*	37, 17, 20	12, 26, 22	11, 15, 18
no. reflns measd	17007	22444	9461
no. unique reflns	6404	7537	5695
no. reflns with $F^2 > 2\sigma(F^2)$	4400	5844	5265
transmission coeff range	0.590−0.862	0.832−0.928	0.686−0.862
R_{int} (on F^2)	0.0394	0.0260	0.0156
weighting params[a] *a*, *b*	0.0494, 0	0.0469, 0	0.0435, 0.6001
R[b]	0.0404	0.0321	0.0298
R_w[c]	0.0983	0.0784	0.0804
no. of params	329	373	325
GOF[d] on F^2	1.009	1.007	1.055
max, min diff map, e Å^{-3}	0.616, −0.395	0.549, −0.347	0.540, −0.370

[a] $w^{-1} = \sigma^2(F_o^2) + (aP)^2 + bP$, where $P = (F_o^2 + 2F_c^2)/3$. [b] Conventional $R = \sum||F_o| - |F_c||/\sum|F_o|$. For "observed" reflections having $F_o^2 > 2\sigma(F_o^2)$. [c] $R_w = [\sum w(F_o^2 - F_c^2)^2/\sum w(F_o^2)^2]^{1/2}$ for all data. [d] GOF = $[\sum w(F_o^2 - F_c^2)^2/(\text{no. unique reflns} - \text{no. of params})]^{1/2}$.

deactivated with 6% w/w water prior to loading. Bu^{t}N≡C was purchased from Aldrich Chemical Co. and used without further purification. The diiron complex $[Fe_2(CO)_6(\mu\text{-}PPh_2)\{\mu\text{-}\eta^1\text{:}\eta^2\text{-}(H)C{=}C{=}CH_2\}]$ was prepared as previously described.[26]

Synthesis of $[Fe_2(CO)_6(\mu\text{-}PPh_2)\{\mu\text{-}\eta^1\text{:}\eta^1\text{-}(Bu^tN{\equiv}C)C{=}CCH_3\}]$ (2) and $[Fe_2(CO)_6(\mu\text{-}PPh_2)(\mu\text{-}\eta^1\text{:}\eta^2\text{-}\{NHBu^tC(O)CH_2\}C{=}CH_2)]$ (3). A diethyl ether solution of Bu^{t}N≡C (0.045 mL, 0.4 mmol) and **1** (0.200 g, 0.4 mmol) was stirred for 60 h, during which time the solution turned from yellow-orange to dark brown. The solvent was removed under reduced pressure to leave a dark brown residue, which was dissolved in the minimum amount of dichloromethane, absorbed onto deactivated alumina, dried, placed on a 300 × 30 mm alumina column, and eluted with petroleum ether/dichloromethane (80:20, v/v). The first band to elute was collected and crystallized from toluene to give **2** as yellow crystals in 15% yield (0.035 g). The second major band was collected and crystallized from *n*-hexane to give **3** as a fine yellow power in 30% yield (0.072 g).

Compound 2: IR (*ν*(CO), cm^{-1}, C_6H_{14}): 2046 s, 2004 s, 1998 s, 1952 m, 1938 w. $^{31}P\{^1H\}$ (202.5 MHz, $CDCl_3$, *δ*): 192.0 (s, *μ*-PPh_2). ^1H NMR (500.1 MHz, $CDCl_3$, *δ*): 7.71−7.13 (m, 10H, C_6H_5), 2.09 (d, 3H $^4J_{PH}$ = 1.8 Hz, C=C−CH_3), 1.33 (s, 9H, $C(CH_3)_3$). $^{13}C\{^1H\}$ NMR (125.7 MHz, $CDCl_3$, *δ*): 249.6 (d, $^2J_{PC}$ = 11.3 Hz, C=*C*−CH_3), 214.9 (s, *C*O), 213.8 (d, $^2J_{PC}$ = 27.3 Hz, *C*O), 211.5 (s, *C*O), 142.8−127.6 (m, C_6H_5), 107.4 (s, *C*≡N), 87.5 (s, *C*=C−CH_3), 60.0 (s, $C(CH_3)_3$), 39.3 (s, C=C−*C*H_3), 30.2 (s, $C(CH_3)_3$). Anal. Calcd for $C_{26}H_{22}Fe_2NO_6P$: N, 2.39; C, 53.19; H, 3.78. Found: N, 2.33, C; 53.01; H, 3.49.

Compound 3: IR (*ν*(CO), cm^{-1}, C_6H_{14}): 2065 w, 2060 w, 2027 s, 1988 s, 1691 w. $^{31}P\{^1H\}$ (202.5 MHz, $CDCl_3$, *δ*): 173.1 (s, *μ*-PPh_2). ^1H NMR (500.1 MHz, $CDCl_3$, *δ*): 7.51−7.18 (m, 10H, C_6H_5), 5.55 (s, 1H, N*H*) 4.00 (d, $^4J_{PH}$ = 12.8 Hz, 1H, C$H_c$$H_d$C(O)NHBu^t), 3.00 (dd, $^4J_{PH}$ = 12.8 Hz, $^4J_{HH}$ = 2.8 Hz, 2H, CH_cH_dC(O)NHBu^t and C=C$H_a$$H_b$), 2.27 (d, $^3J_{PH}$ = 10.1 Hz, $^4J_{HH}$ = 2.8 Hz, 1H, C=C$H_a$$H_b$) 1.35 (s, 9H, $C(CH_3)_3$). $^{13}C\{^1H\}$ NMR (125.7 MHz, $CDCl_3$, *δ*): 212.1 (s, *C*O), 180.4 (d, $^2J_{PC}$ = 21.7 Hz, CH_2=*C*−CH_2), 169.3 (s, *C*(O)NHBu^t), 138.8−127.5 (m, C_6H_5), 72.4 (d, $^2J_{PC}$ = 14.6 Hz, CH_2=C−CH_2), 67.3 (d, $^3J_{PC}$ = 2.9 Hz, CH_2=C-*C*H_2), 51.5 (s, *C*$(CH_3)_3$), 28.5 (s, C$(CH_3)_3$). Anal. Calcd for $C_{26}H_{24}Fe_2NO_7P$: N, 2.31; C, 51.60; H, 4.00. Found: N, 2.26, C; 51.87; H, 3.96. MS (EI): *m*/*z* 576 (M^+ − CO), 549 (M^+ − 2CO), 521 (M^+ − 3CO), 493 (M^+ − 4CO), 465 (M^+ − 5CO), 437 (M^+ − 6CO).

Synthesis of $[Fe_2(CO)_6(\mu\text{-}PPh_2)\{\mu\text{-}\eta^1\text{:}\eta^1\text{-}||\text{-}C(Bu^tNH)(NHPr^i)C{=}CCH_3\}]$ (4). Addition of excess NH_2Pr^i (1.0 mL, 11.41 mmol) to a hexane solution of $[Fe_2(CO)_6(\mu\text{-}PPh_2)\{\mu\text{-}\eta^1\text{:}\eta^1\text{-}(Bu^tN{\equiv}C)C{=}CCH_3\}]$ (0.110 g 0.19 mmol) resulted in the immediate precipitation of a pale yellow solid. After stirring overnight the reaction mixture was filtered and the resulting solid washed with 2 × 10 mL portions of hexane to afford **4** as an analytically pure solid (0.100 g, 91%). IR (*ν*(CO), cm^{-1}, CH_2Cl_2): 2031 m, 1984 s, 1959 s, 1932 w, 1915 w. $^{31}P\{^1H\}$ (121.0 MHz, $CDCl_3$, *δ*): 191.7 (s, *μ*-PPh_2). ^1H NMR (500.1 MHz, $CDCl_3$, *δ*): ^1H NMR (500.1 MHz, $CDCl_3$, *δ*): 7.82−7.79 (m, 2H, C_6H_5), 7.61 (t, $^3J_{HH}$ = 8.0 Hz, 2H, C_6H_5), 7.39−7.12 (m, 6H, C_6H_5), 4.81 (d, $^3J_{HH}$ = 9.8 Hz, N*H*Pr^i), 3.88 (br m, 1H, NHC*H*$(CH_3)_2$), 3.85 (s, 1H, N*H*Bu^t), 1.75 (s, 3H, C=CCH_3), 1.20 (d, $^3J_{HH}$ = 6.4 Hz, 3H, CHC$H_3$$(CH_3)$), 1.05 (d, $^3J_{HH}$ = 6.4 Hz, 3H, $CHCH_3$(CH_3)), 1.00 (s, 9H, C(CH_3)$_3$). $^{13}C\{^1H\}$ NMR (125.65 MHz, $CDCl_3$, *δ*): 217.6 (d, $^2J_{PC}$ = 8.4 Hz, *C*O), 216.0 (d, $^2J_{PC}$ = 38.6 Hz, *C*O) 211.6 (d, $^2J_{PC}$ = 14.2 Hz, *C*O) 167.3 (s, C=*C*−CH_3), 161.0 (d, $^2J_{PC}$ = 11.3 Hz, *C*=C−CH_3), 144.7 (d, $^1J_{PC}$ = 18.3 Hz, C_6H_5), 142.9 (d, $^1J_{PC}$ = 26.1 Hz, C_6H_5), 133.6−127.6 (m, C_6H_5), 121.1 (d, $^3J_{PC}$ = 8.9 Hz, N−*C*−N), 51.9 (s, *C*$(CH_3)_3$), 47.0 (s, *C*H$(CH_3)_2$), 31.2 (s, C=C−*C*H_3), 29.1 (s, C$(CH_3)_3$), 24.1 (s, CH*C*$H_3$$(CH_3)$), 23.6 (s, $CHCH_3$(*C*H_3)). Anal. Calcd for $C_{29}H_{31}Fe_2N_2O_6P$: N, 4.33; C, 53.87; H, 4.83. Found: N, 4.40, C; 53.92; H, 4.82.

Synthesis of 5, $[Fe_2(CO)_5(\mu\text{-}PPh_2)(\mu\text{-}\eta^1\text{:}\eta^2\text{-}\{NHBu^tC(O)CH_2\}C{=}CH_2)]$. Complex **3** (0.140 g, 0.21 mmol) was dissolved in 30 mL of toluene or $CDCl_3$ and the solution left to stir under an inert atmosphere for several days, during which time the reaction mixture turned from deep yellow to bright red. The solvent was removed to give a red solid, which was dissolved in dichloromethane, absorbed onto deactivated alumina, placed on a 300 × 30 mm column, and eluted with *n*-hexane/dichloromethane (50:50, v/v). A single major red

band eluted, which was collected and crystallized from petroleum ether/dichloromethane to give red crystals of **5** in 95% yield (0.126 g). IR (ν(CO), cm^{-1}, C_6H_{14}): 2029 w, 1996 s, 1959 m, 1945 w, 1617 w. $^{31}P\{^1H\}$ (202.5 MHz, $CDCl_3$, δ): 173.0 (s, μ-PPh_2). ^1H NMR (200.1 MHz, $CDCl_3$, δ): 7.0−7.6 (m, 10H, C_6H_5), 5.80 (br, 1H, N*H*) 4.23 (d, $^2J_{PH}$ = 19.1 Hz, 1H, C$H_c$$H_d$C(O)NHBu^t), 3.18 (dd, $^3J_{PH}$ = 11.6 Hz, $^2J_{HH}$ = 2.6 Hz, 1H, C=C$H_a$$H_b$), 2.78 (dd, $^3J_{PH}$ = 19.1 Hz, $^2J_{HH}$ = 2.6 Hz, 1H, CH$_c$$H_d$C(O)NHBu^t), 2.21 (d, $^3J_{PH}$ = 7.0 Hz, 1H, C=CH$_a$$H_b$), 1.21 (s, 9H, NC(C$H_3$)$_3$). $^{13}C\{^1H\}$ NMR (125.7 MHz, $CDCl_3$, δ): 218.7 (d, $^2J_{PC}$ = 12.0 Hz, *C*O), 215.7 (d, $^2J_{PC}$ = 3.0 Hz, *C*O), 213.5 (d, $^2J_{PC}$ = 15.0 Hz, *C*O), 183.1 (s, *C*(O)NHBu^t), 168.0 (d, $^2J_{PC}$ = 27.0 Hz, H$_2$C=*C*CH$_2$C(O)NHBu^t), 125.0−140.0 (m, C_6H_5), 63.2 (d, $^2J_{PC}$ = 8.7 Hz, H$_2$*C*=CCH$_2$C(O)NHBu^t), 57.9 (d, $^3J_{PC}$ = 4.6 Hz, H$_2$C=C*C*H$_2$C(O)NHBu^t), 53.0 (s, C(O)*C*(CH$_3$)$_3$), 28.5 (s, C(O)C(*C*H$_3$)$_3$). 14.6 Hz, *C*H$_2$=C−CH$_2$), 67.3 (d, $^3J_{PC}$ = 2.9 Hz, CH$_2$=C−*C*H$_2$), 51.5 (s, *C*(CH$_3$)$_3$), 28.5 (s, C(*C*H$_3$)$_3$). Anal. Calcd for $C_{25}H_{24}Fe_2NO_6P$: N, 2.43; C, 52.02; H, 4.19. Found: N, 2.39, C; 51.81; H, 3.85.

Crystal Structure Determination of 2, 4, and 5. All measurements were made on a Bruker AXS SMART CCD area-detector diffractometer using graphite-monochromated Mo Kα radiation (λ = 0.71073 Å) and narrow frame exposure (0.3° in ω). Cell parameters were refined from the observed ω angles of all strong reflections in each data set. Intensities were corrected semiempirically for absorption, based on symmetry-equivalent and repeated reflections. No significant intensity decay was observed. The structures were solved by direct methods and refined on F^2 values for all unique data by full-matrix least-squares. Table 2 gives further details. All non-hydrogen atoms were refined anisotropically. H atoms, located in difference maps, were constrained with a riding model except for those attached to N(1) and N(2) in **4**, and C(1) in **5**, which had their coordinates freely refined because of nonstandard geometry; U(H) was set at 1.2 (1.5 for methyl groups) times U_{eq} for the parent atom. Programs used were SHELXTL[27] for structure solution, refinement, and molecular graphics, Bruker AXS SMART (control) and SAINT (integration), and local programs.[28]

Acknowledgment. We thank the University of Newcastle upon Tyne for financial support, the Nuffield Foundation and the Royal Society for grants (S.D.), and the EPSRC for funding for a diffractometer (W.C.).

Supporting Information Available: For **2**, **4**, and **5** details of structure determination, non-hydrogen atomic positional parameters, full listings of bond distances and angles, anisotropic displacement parameters, and hydrogen atomic coordinates. This material is available free of charge via the Internet at http://pubs.acs.org. Observed and calculated structure factor tables are available from the authors upon request.

OM9901630

(27) Sheldrick, G. M. *SHELXTL user manual, version 5*; Bruker AXS Inc.: Madison, WI, 1994.

(28) SMART and SAINT software for CCD diffractometers; Bruker AXS Inc.: Madison, WI, 1994.